ANL/ET/CP--81785
Conf-930928--27

CREEP PROPERTIES OF VANADIUM-BASE ALLOYS *

by

H. M. Chung, B. A. Loomis, and D. L. Smith
Argonne National Laboratory
Argonne, IL 60439 U.S.A.

December 1993

RECEIVED
FEB 16 1994
OSTI

DISCLAIMER

MASTER

To be published in the Proceedings of the Sixth International Conference on Fusion Reactor Materials, September 27-October 1, 1993, Stresa, Italy.

---

* Work supported by the U.S. Department of Energy, Office of Fusion Energy, under Contract W-31-109-Eng-38.

DISTRIBUTION OF THIS DOCUMENT IS UNLIMITED

Creep properties of vanadium-base alloys*

H. M. Chung, B. A. Loomis, and D. L. Smith
Argonne National Laboratory, Argonne, IL 60439, U.S.A.
e-mail hee_chung@qmgate.anl.gov, fax 1 708 252 3604, tel. 1 708 252 5111

Vanadium-base alloys are promising candidate materials for application in fusion reactor structural components because of several important advantages. V-4Cr-4Ti has been identified as one of the most promising candidate alloys and was selected for comprehensive tests and examination. In the present investigation, thermal creep rates and stress-rupture life of V-4Cr-4Ti and V-10Cr-5Ti alloys were determined at 600°C. The impurity composition and microstructural characteristics of creep-tested specimens were analyzed and correlated with the measured creep properties. The results of these tests show that V-4Cr-4Ti, which contains impurity compositions typical of a commercially fabricated vanadium-based alloy, exhibits creep strength substantially superior to that of V-20Ti, HT-9, or Type 316 stainless steel. The V-10Cr-5Ti alloy exhibits creep strength somewhat higher than that of V-4Cr-4Ti.

1. Introduction

Vanadium-base alloys are considered promising candidate structural materials for a fusion reactor first wall because they offer the important advantages of inherently low irradiation-induced activity, good mechanical properties, good compatibility with lithium, high thermal conductivity, and good resistance to irradiation damage. As part of a program to screen candidate alloys and develop an optimal alloy, extensive investigations have been conducted on the swelling behavior, tensile properties, impact toughness, and microstructural evolution of V, V-Ti, V-Cr, V-Cr-Ti, and V-Ti-Si alloys after irradiation by fast neutrons at 420, 520, and 600°C. From these investigations, V-Cr-Ti alloys containing 5-7 wt.% Cr, 3-5 at.% Ti, 400-1000 wt. ppm Si, and <1000 wt. ppm O+N+C were identified as desirable alloys that exhibit superior resistance to swelling, embrittlement, and hydrogen-induced effects during irradiation in lithium [1-4]. As a result, recent attention has focused primarily on the ternary alloys V-4Cr-4Ti, V-5Cr-3Ti, and V-5Cr-5Ti. For these alloys, however, no data base has been reported on thermal or irradiation creep, and a favorable creep behavior commensurate with the superior resistance of the alloys to swelling and embrittlement has not been demonstrated. In the work reported here, the thermal creep behavior of a V-4Cr-4Ti alloy was investigated at 600°C. The creep of V-10Cr-5Ti was also investigated to provide information on the effect of increased Cr content. Preliminary results of the creep tests have been described in a previous report [5].

2. Materials and procedures

---

* Work supported by the Office of Fusion Energy, U.S. Department of Energy, under Contract W-31-109-Eng-38.

The chemical composition of the two alloys tested in the present investigation is given in Table 1. The 0.635-mm-thick tensile specimens were recrystallized prior to the creep test by annealing at 1125°C for 1 h in a vacuum of 2 x 10-5 Pa. The creep tests were conducted in an ion-pumped system in which vacuum was typically maintained at 2 x 10^{-6} Pa during testing at 600°C. Details of experimental procedures have been reported elsewhere [5]. The specimen was wrapped with a Ti or Ta foil to reduce contamination with impurities during testing. The elongation of a specimen was determined with a linear variable differential transformer (LVDT) with digitized output. The concentration of interstitial impurities (i.e., O, N, and C) and hardness (VHN) of specimens were measured after testing. The phase and dislocation structures of the specimens were examined by transmission electron microscopy (TEM) before and after the creep test. In addition to the normal constant-load stress-to-rupture tests, applied stress was increased stepwise in some tests to measure a set of steady-state (minimum) creep rates corresponding to each stress level. An example of this kind of testing is shown in Fig. 1.

Table 1. Chemical Composition of V-4Cr-4Ti and V-10Cr-5Ti Alloys

		Composition (wt.% or wt ppm)					
Material	ANL ID	Cr	Ti	Si	O	C	N
V-4Cr-4Ti	BL-47	4.1%	4.3%	870	350	200	220
V-10Cr-5Ti	BL-43	9.2%	4.9%	340	230	100	31

[a] Annealed at 1125°C for 1 h.

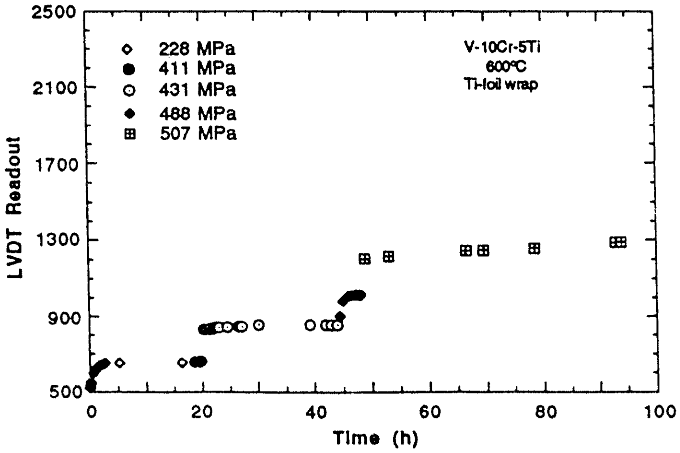

Fig. 1. Elongation (LVDT readout) vs. time for V-10Cr-5Ti under stepwise increase in loading at 600°C, used to measure steady-state creep rates.

3. Results and discussion

3.1 Stress-rupture life and creep rate

The stress-to-rupture time of V-4Cr-4Ti and V-10Cr-5Ti is given in Fig. 2. The figure shows that the creep strength of the V-10Cr-5Ti alloy is significantly higher (≈100 MPa) than that of V-4Cr-4Ti. This finding is consistent with the higher ultimate tensile strength (UTS) of V-10Cr-5Ti, i.e., ≈512 vs. ≈434 MPa [6]. At 600°C, the stress-to-rupture time of the two alloys is extremely sensitive to applied stress. For example, an increase in rupture time of more than two orders of magnitude was observed for V-4Cr-4Ti when applied stress was decreased only ≈5%. In previous investigations of creep properties of V-13Cr-3Ti, V-15Cr-3Ti, V-15Cr-5Ti, and Vanstar alloys at ≥650°C, a similar trend was observed [7-9]. Because of the high creep strength, determination of stress-rupture life of V-5Cr-5Ti at 600°C for stress ≤350 MPa is estimated to require impractically long test times (≥3 years).

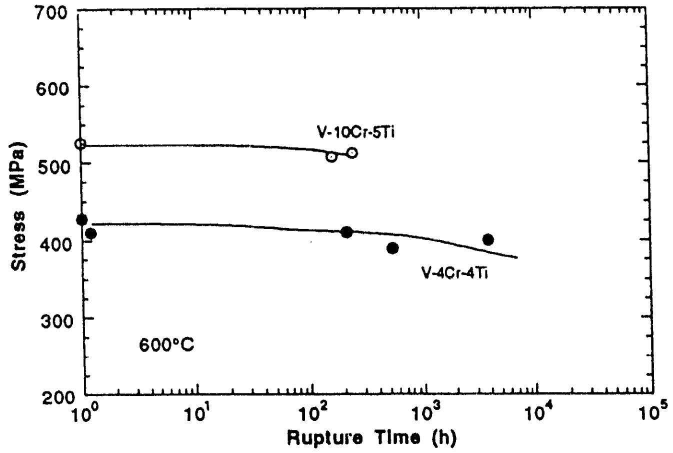

Fig. 2. Relationship of stress to rupture time for V-10Cr-5Ti and V-4Cr-4Ti at 600°C.

In Fig. 3, steady-state (minimum) creep rates of V-4Cr-4Ti and V-10Cr-5Ti alloys are shown as a function of applied stress. In the stress range between ≈300 and ≈420 MPa, the steady-state creep rate of V-4Cr-4Ti at 600°C was between $\approx 10^{-3}$ and 5×10^{-2} %/h; for a comparable stress level, creep rate of V-10Cr-5Ti was ≈7-8 times lower.

In Fig. 4, the creep strengths of V-15Cr-5Ti, V-10Cr-5Ti, and V-5Cr-5Ti are given. Although data for V-15Cr-5Ti were obtained at temperatures higher than 600°C [9], the creep strengths can be compared from a plot of the Larsen-Miller parameter, which is defined by the equation:

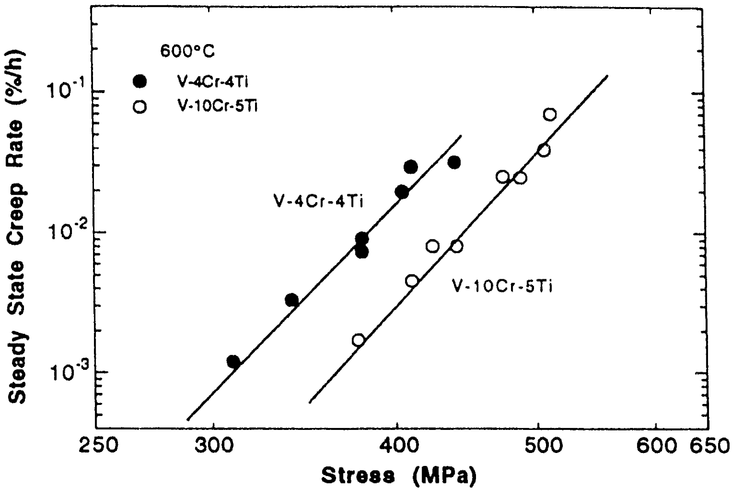

Fig. 3. Steady-state creep rate vs. stress for V-10Cr-5Ti and V-4Cr-4Ti at 600°C.

$$P = T(20 + \log t), \quad (1)$$

where creep temperature T is in K and rupture time t is in hours. The V-15Cr-5Ti specimens tested by Bajaji and Gold [9] contained 200-1400 wppm O, 500 wppm N, and 170 wppm C. By comparison, the impurity content measured in the creep-tested specimens of V-10Cr-5Ti and V-4Cr-4Ti in the present investigation were significantly lower: i.e., O, 370-770 wppm; N, 99-200 wppm; and C, 252-270 wppm (see Table 2). Within the uncertainties associated with the variations in impurity content, the results indicate that the creep strengths of V-15Cr-5Ti and V-10Cr-5Ti are similar. The UTS of the present V-10Cr-5Ti (541 MPa) and that of a V-15Cr-5Ti alloy containing 400 wppm O, 490 wppm N, and 280 wppm C was found to be similar (555 MPa). Therefore, it is not surprising that the creep strengths of V-10Cr-5Ti and V-15Cr-5Ti, shown in Fig. 3, are similar.

3.2 *Impurity content and microstructure*

The creep of unalloyed V is known to be sensitive to impurities (in particular dissolved O), although the creep of V-15Cr-5Ti, V-20Ti, and Vanstar-7 (V-9Cr-3Fe-1.3Zr-0.05C) appears to be less sensitive to O contamination (see Fig. 4) [7-9]. In view of this, it was considered necessary to characterize the specimen impurity content, hardness, phase distribution, and other undesirable microstructural changes associated with the creep test to qualify the data obtained in this study.

The results obtained from analysis for O, N, and C concentrations are summarized in Table 2. Compared with the impurity content of the as-annealed specimens before the test (Table 1), N content in V-4Cr-4Ti decreased to some extent (from 220 to 160-190 wppm) and C content increased modestly (from 200 to 250-270 wppm). Nitrogen content in V-10Cr-5Ti increased from 31 to ≈100 wppm. However, the O content of both alloys increased significantly after testing (from 230-350 wppm to 370-770 wppm). The increase in O content was more pronounced in specimens tested without a wrap or with a Ta-foil wrap. For a specimen with a Ti wrap, the increase in O content was minimal (e.g., from 230 to 370 wppm). The more pronounced O contamination in the Ta-wrapped specimens is probably associated with the volatility of tantalum oxide. Because of the smaller contamination when Ti foil was used, all subsequent tests are being conducted with a Ti wrap. Despite the increase in O and C, the impurity content of the two alloys is still comparable to that typical of a commercial V-base alloy.

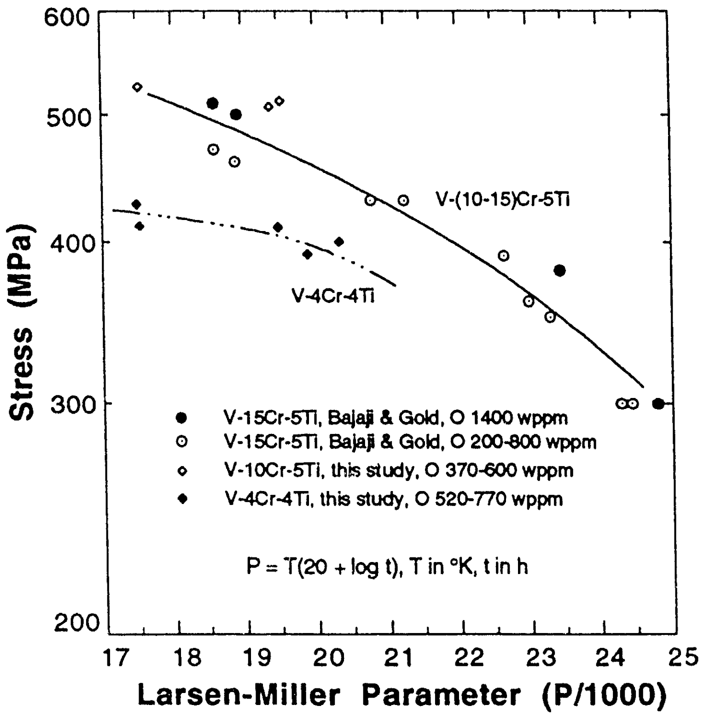

Fig. 4. Larsen-Miller plots for V-15Cr-5Ti, V-10Cr-5Ti, and V-4Cr-4Ti.

Table 2. Impurity Content of Creep Specimens from V-4Cr-4Ti[a] and V-10Cr-5Ti[b] after Testing at 600°C.

Material	Specimen ID	Stress (MPa)	Time to Rupture (h)	Wrap	Composition (wt ppm)		
					O	C	N
V-4Cr-4Ti	BL-47A	420	1	none	560	252	160
V-4Cr-4Ti	BL-47C	408	1.1	Ta	520	261	200
V-4Cr-4Ti	BL-47E	387	541	Ta	770	-	200
V-4Cr-4Ti	BL-47F	410	213	Ta	520	270	190
V-10Cr-5Ti	BL-43A	512	243	none	600	-	120
V-10Cr-5Ti	BL-43B	507	162	Ti	370	-	99

[a] Ultimate tensile strength ≈434 MPa, hardness VHN ≈171.

[b] Ultimate tensile strength ≈512 MPa, hardness VHN ≈192.

To detect undesirable phase structure that might have been produced during testing, TEM specimens excised from near the gage section were examined. The results are shown in Fig. 5. A comparison of Figs. 5A and 5B shows that the phase structure of V-4Cr-4Ti did not change appreciably during testing at 600°C for 541 h. That is, the size and distribution of the Ti(O,N,C) precipitates, normally observed in these alloys after fabrication [3], were similar before and after testing, and no new types of precipitates were produced.

However, dislocation loops were observed in high density in creep-tested specimens of both V-4Cr-4Ti and V-10Cr-5Ti (Figs. 5C and 5D, respectively). From bright-field imaging alone, the dislocation loops (≤100 nm in size) can be mistakenly confused with small precipitates. However, results of selected-area diffraction and dark-field imaging showed that they are indeed dislocation loops. Line dislocations were also observed frequently in conjunction with loops (Fig. 5E). A major difference in the microstructural aspect of creep-tested V-4Cr-4Ti and V-10Cr-5Ti specimens was the distribution of dislocation loops. In V-10Cr-5Ti, loop distribution was more or less uniform within a grain. In contrast, size and density of the loops were higher near a grain boundary in V-4Cr-4Ti. This can be seen by comparing the two bright-field images of Figs. 5C and 5D. The dark-field image shown in Fig. 5F reveals more clearly a dense loop distribution of V-4Cr-4Ti in the vicinity of a grain boundary.

Hardness profiles were measured across the specimen thickness (nominal thickness 0.635 mm) after the creep test. An example of typical hardness profiles is given in Fig. 6, which was determined for a V-10Cr-5Ti specimen that ruptured after 162 h. Except for narrow regions ≤0.01 mm underneath the free surfaces, a more or less uniform hardness of ≈205 VHN was observed, a slight increase from the original hardness of ≈192 VHN. The hardness increase is attributed not only to the effect of the increase in O content (i.e., from 230 to 370 wppm) but also to the effect of the high-

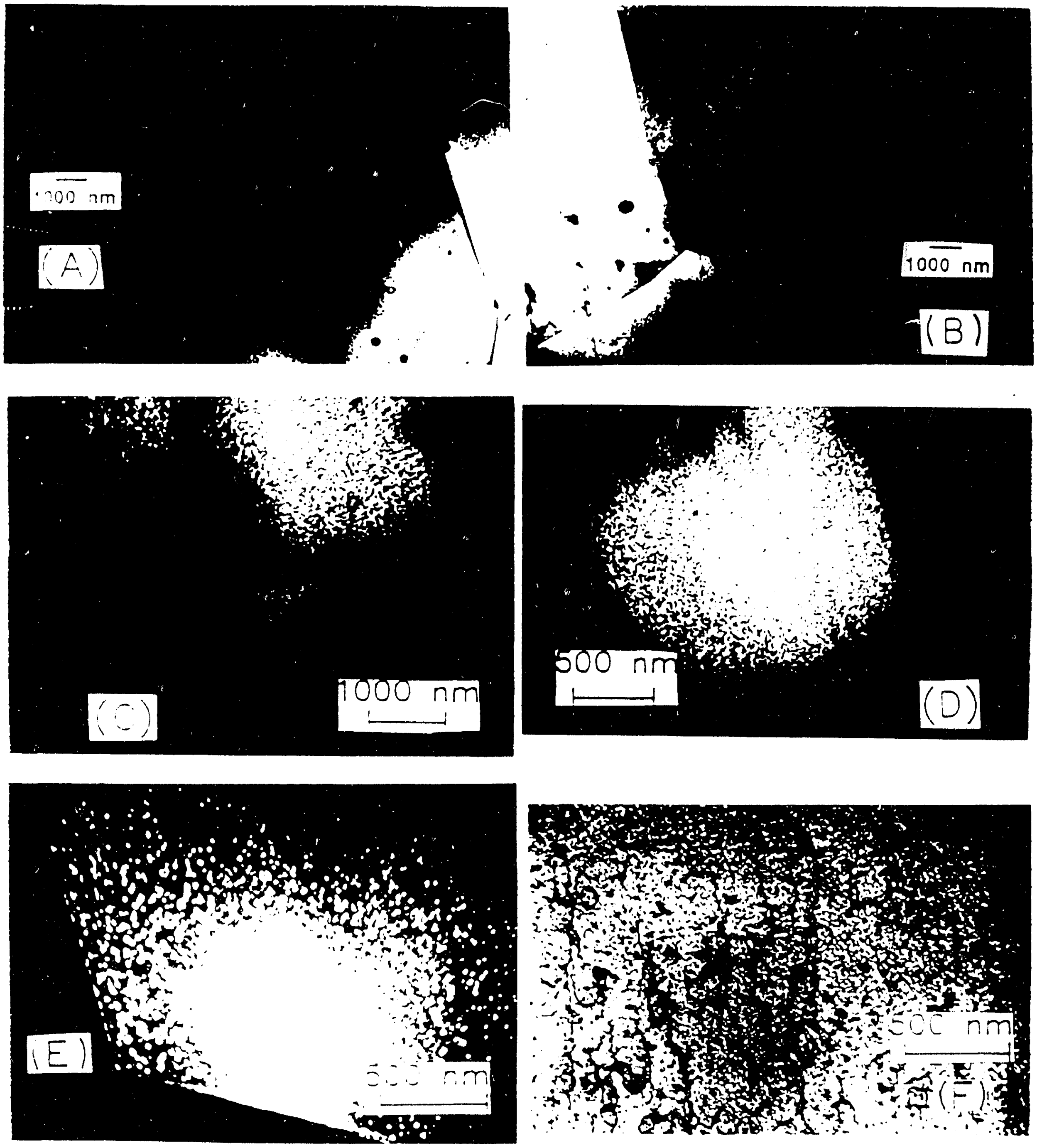

Fig. 5. Phase structure of V-4Cr-4Ti (A) before and (B) after creep test at [illegible] °C for 541 h; (C) dislocation loops in the specimen shown in (B) and (D) dislocation loops in V-10Cr-5Ti after test at [illegible] °C for [illegible] h; (E) dark-field image of loop distribution of (C); and (F) bright-field image of dislocations and dislocation loops of (C).

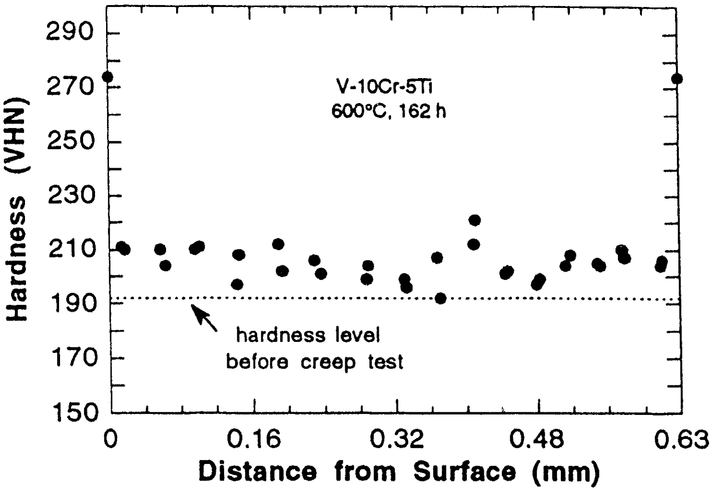

Fig. 6. Vickers hardness profile across wall thickness of V-10Cr-5Ti after creep test at 600°C for 162 h.

density dislocation loops. In summary, no unusual features were observed that indicate an unacceptable effect of the environment of the creep test at 600°C. Impurity content and phase structure of the test specimens were similar to those of typical commercial alloys.

3.3 *Comparison with Other Materials*

In Fig. 7, the creep property of V-4Cr-4Ti and ferritic and austenitic steels is shown in Larsen-Miller plots. From the figure, it is obvious that the creep strength of V-4Cr-4Ti is substantially superior to that of HT-9, Type 316 stainless steel, and V-20Ti. In particular, this difference in creep strength is more pronounced when Larsen-Miller parameters are higher, i.e., at higher temperatures or longer times.

It has been reported that creep strength of binary V-Ti and ternary V-15Cr-Ti and V-3Cr-Ti alloys is maximum for 3 wt.% Ti [7,8]. Titanium content greater or less than ≈3 wt.% resulted in significantly decreased creep strength. Based on this observation, the creep strength of V-5Cr-3Ti is expected to be substantially higher than that of V-4Cr-4Ti. Increasing the Cr content to 7 wt.% is also expected to improve the creep strength of V-4Cr-4Ti. However, selection of optimal content of Cr (5-7 wt.%) and Ti (3-5 wt.%) must be tied closely to other important considerations, in particular, to the effects of neutron damage and He generation on embrittlement and fracture toughness.

4. Conclusions

1. Stress-rupture life and steady-state creep rate of V-4Cr-4Ti and V-10Cr-5Ti have been determined

at 600°C. Results of characterization of impurity contamination, hardness, phase structure, and dislocation and loop structures in the creep-tested specimens showed no unusual features that indicate an unacceptable effect of the test environment on the measured creep rates. Impurity content of the tested specimens was comparable to that of a typical commercial vanadium-base alloy.

2. V-4Cr-4Ti exhibits a creep strength that is substantially superior to that of Type 316 stainless steel, HT-9, or V-20Ti, in particular, at higher Larsen-Miller parameters, i.e., at higher temperatures and/or longer service times.
3. Creep strength of V-10Cr-5Ti is similar to that of V-15Cr-5Ti and several times higher than that of V-4Cr-4Ti. However, if a creep strength higher than that of V-4Cr-4Ti is required, V-5Cr-3Ti or V-7Cr-5Ti appears to be a more attractive alternative than V-10Cr-5Ti from the standpoint of irradiation-induced embrittlement.

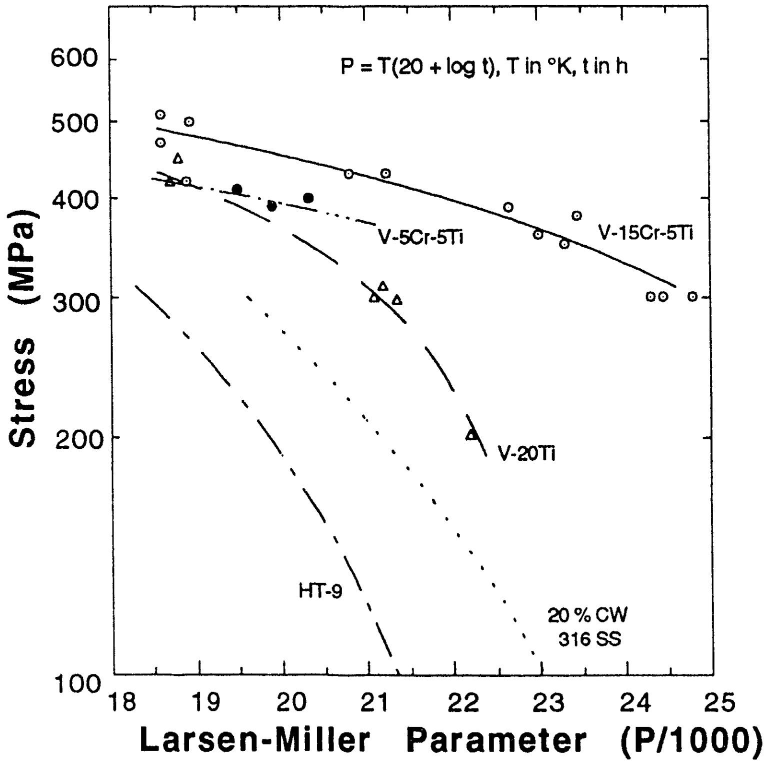

Fig. 7. Larsen-Miller plots of creep strength of V-4Cr-4Ti and ferritic and austenitic steels.

Acknowledgments

The authors are grateful to L. J. Nowicki and J. Gazda for their contributions to experimental efforts. This work was supported by the Office of Fusion Energy, U. S. Department of Energy, under Contract W-31-109-Eng-38. The authors thank Dr. F. W. Wiffen for helpful discussions.

References

[1] B. A. Loomis, A. B. Hull, and D. L. Smith, J. Nucl. Mater., 179-181 (1991) 148-154.

[2] B. A. Loomis and D. L. Smith, J. Nucl. Mater., 191-194 (1992) 84-91.

[3] H. M. Chung and D. L. Smith, J. Nucl. Mater. 191-194 (1992) 942-947.

[4] H. M. Chung, B. A. Loomis, and D. L. Smith, "Irradiation-Induced Precipitation in Vanadium-Base Alloys Containing Titanium," in: Effects of Radiation on Materials: 16th International Symposium, ASTM STP 1175, A. S. Kumar, D. S. Gelles, R. K. Nanstad, and T. A. Little, eds., American Society for Testing and Materials, Philadelphia, 1993.

[5] B. A. Loomis, L. J. Nowicki, and D. L. Smith, in: Fusion Reactor Materials, Semiannual Progress Report for Period Ending September 30, 1992, DOE/ER-0313/13, U.S. Department of Energy, Office of Fusion Energy, in press.

[6] B. A. Loomis, L. J. Nowicki, and D. L. Smith, in: Fusion Reactor Materials, Semiannual Progress Report for Period Ending March 31, 1991, DOE/ER-0313/10, U.S. Department of Energy, Office of Fusion Energy, July 1991, pp. 145-155.

[7] M. Schirra, "Das Zeitstandfestigkeits und Kriechverhalten von Vanad-Basis Legierungen," KfK-2440, April 1977, Karlsruhe Nuclear Research Center, Germany.

[8] D. Harrod and R. Gold, "Mechanical Properties of Vanadium and Vanadium Base Alloys," Int. Met. Rev. 25 (1980) 163-221.

[9] R. Bajaji and R. E. Gold, in: Alloy Development for Irradiation Performance Semiannual Progress Report, DOE/ER0045/10, Oak Ridge National Laboratory, Oak Ridge, TN, 1983, p. 74.

END

DATE FILMED

3/15/94